

110412

TRANSITION FROM THE SECTOR ZONE TO THE UNIPOLAR ZONE IN THE HELIOSHEATH:
VOYAGER 2 MAGNETIC FIELD OBSERVATIONS

L. F. Burlaga¹ and N. F. Ness²

¹ NASA Goddard Space Flight Center, Code 673, Greenbelt, MD 20771, USA;

lburlagahsp@verizon.net

² Institute for Astrophysics and Computational Sciences, Catholic University of America,

Washington, DC 20064, USA: nfnudel@yahoo.com

ABSTRACT

The magnetic polarity pattern observed by *Voyager 2* (*V2*) evolved with time from a nearly equal mixture of positive and negative polarity sectors in the sector zone from 2007.00 to 2007.67 to nearly uniform positive polarity (magnetic fields directed away from the Sun) in the unipolar zone from 2009.6 to 2010.3. This change was caused by the decreasing latitudinal extent of the sector zone, when the minimum extent of the heliospheric current sheet moved northward toward the solar equator as the solar activity associated with solar cycle 23 decreased a minimum in 2010. In the heliosheath, the distribution of daily averages of the magnetic field strength B was lognormal in the sector zone from 2008.83 to 2009.57 and Gaussian in the unipolar zone from 2009.57 to 2010.27. The distribution of daily increments of B was a Tsallis distribution (q -Gaussian distribution) with $q = 1.66 \pm 0.010$ in the sector zone and \approx Gaussian ($q = 1.01 \pm 0.29$) in the unipolar zone. The unipolar region appears to be in a relatively undisturbed equilibrium state.

Key words: solar wind-Sun: Heliosphere

1. INTRODUCTION

This paper discusses observations of magnetic fields when the spacecraft *Voyager 2* (V2) left the supersonic solar wind from 2007.00 to 2007.67, crossed the termination shock (TS) at 2007.67, and moved through the heliosheath from 2007.67 to 2010.27. Section 2 describes the evolution of the magnetic polarity observed by V2 from 2007.00 to 2010.27, when the spacecraft moved from 81.6 AU - 91.6 AU and from 27.1° - 28.9° S latitude. From the 2007.00 to 2007.67, V2 was in the "sector zone" in the supersonic solar wind measuring positive and negative magnetic polarity with nearly equal probability. From 2007.67 to 2009.56, V2 remained in the sector zone, but the magnetic polarity became increasingly positive. From 2009.57 to 2010.27 V2 observed positive polarity at least 95% of the time; hence, V2 was in the "unipolar zone". In Section 3 the distribution of daily averages of the magnetic field strength B in the sector zone is compared with that in the unipolar zone. In Section 4 the distribution of increments of daily averages of B observed in the sector zone is compared with that observed in the unipolar zone.

2. MAGNETIC POLARITY OBSERVED BY VOYAGER 2

A pattern of alternating positive and negative magnetic polarities (the "sector pattern") is often observed by spacecraft near the ecliptic. Reviews of the sector structure in the supersonic solar wind were published by Smith (2001) and Ness & Burlaga (2001). Schatten et al. (1969) suggested that the sector pattern is related to the existence of the Heliospheric Current Sheet (HCS). The HCS is a wavy current sheet, with a maximum

latitudinal extent (Δ_M) in northern hemisphere and a minimum latitudinal extent (Δ_m) in the southern hemisphere, which separates the positive and negative magnetic polarities of the polar magnetic fields of the Sun, and is related to the magnetic neutral line in a spherical source surface near the Sun (Schulz, 1973). The latitudinal extent of the HCS varies with solar cycle from a maximum value near solar maximum and minimum value near solar minimum. The maximum latitudinal extent of the HCS changes little, $< 10^\circ$, from the Sun to at least ~ 98 AU (Burlaga & Ness, 1997; Burlaga et al., 2009). When the latitude of a spacecraft is between the Δ_M and Δ_m , the HCS moves past the spacecraft multiple times and it observes a sector pattern. The range of latitudes in which the sector pattern can be observed by a spacecraft is called the "sector zone" (Burlaga & Ness, 1997, 2003). When a spacecraft is above or below the sector zone, it observes a nearly uniform polarity (+ or -) corresponding to the dominant magnetic polarity of the Sun in that hemisphere. We shall call this region the "unipolar zone".

Wang and Sheeley computed the minimum latitudinal extent of the HCS on a source surface at $2.5 R_s$ (solar radii) for each solar rotation as a function of time by projecting measurements of the photospheric magnetic field using their "radial" model (Wang & Sheeley, 1992). Figure 1 shows the minimum latitudinal extent of the HCS for successive solar rotations projected to the position of V2, assuming radial propagation from the source surface to V2. The points and solid curve in Figure 1 were computed with magnetic field observations from the Mount Wilson Observatory (MWO) and Wilcox Solar Observatory (WSO), respectively. The latitude of V2 as a function of time is shown by the slowly changing smooth curve in Figure 1. The minimum latitudinal extent of the HCS (nearly -90°) for all of the solar rotations shown in Figure 1 occurred during the year 2000 (solar

maximum), and the minimum latitude of the HCS increased with declining solar activity to nearly -30° , close to but still poleward of the latitude of $V2$, at the beginning of 2006. It remained close to the latitude of $V2$, possibly crossing it at times, such as the interval near 2008.0 - 2008.2 in Figure 1, until ~ 2009.6 , when it abruptly moved to latitudes closer to the heliographic equator. Since the HCS was closer to the equator than $V2$ after 2009.6, $V2$ should observe predominantly positive polarity from 2009.6 through at least 2010.27. Since the minimum latitude of the HCS at 1 AU remained within 20° of the heliographic equator through January 1, 2010 (Ahluwalia & Ygbuhay, 2011), and since it takes at least a year for the solar wind to move from 1 AU to $V2$, one expects that $V2$ should have observed positive polarity until at least January 1, 2011, in the absence of other effects such as southward flows in heliosheath. *Voyager 1* did observe a return of the sector pattern in the heliosheath after it left the sector zone (Burlaga & Ness, 2010), probably as a result of northward flows in heliosheath (Borovikov, et al., 2011).

Daily averages of the azimuthal angle λ of the magnetic field \mathbf{B} in HG coordinates observed by $V2$ from 2007.00 to 2010.27 are shown in Figure 2a. The solar wind model of Parker (1963) predicts that in the distant supersonic solar wind $\lambda = 270^\circ$ (positive magnetic polarity) when \mathbf{B} is pointing away from the Sun along the spiral direction, and $\lambda = 90^\circ$ (negative magnetic polarity) when \mathbf{B} is pointing toward the Sun. In general, the angles fluctuate about these two directions owing to both physical effects and uncertainties in the measurements. This same behavior has been observed in the heliosheath (Burlaga & Ness, 2010; Burlaga et al., 2010). In the absence of a suitable calibration of the magnetometers for the radial component of \mathbf{B} , we assume that the average value of the radial component of \mathbf{B} , $\langle BR \rangle_{52}$, is equal to zero during an interval of 52 days centered at the time of a spacecraft

roll. The spacecraft rolls occur every few months. This assumption tends to force the distribution of λ to have peaks near 90° and 270° , but it does not significantly affect the fractions of positive and negative polarities.

Figure 2(a) shows that *V2* observed both negative magnetic polarities ($0^\circ \leq \lambda < 180^\circ$) and positive polarities ($180^\circ \leq \lambda < 360^\circ$) in the supersonic solar wind from 2007.00 to 2007.67 and in the heliosheath from 2007.67 to 2009.57. Figure 2(a) also shows that *V2* observed positive polarities almost exclusively from 2009.6 to 2010.27. A least squares fit to the observations of $\lambda(t)$ using the sigmoid function, $\lambda = A_2 + (A_1 - A_2)/(1 + \exp((t - t_0)/\tau))$, gives a good fit ($R^2 = 0.085$, where R^2 is the coefficient of determination) with the parameters $A_1 = 189^\circ \pm 10^\circ$ (corresponding to a nearly equal mixture of positive and negative polarities), $A_2 = 263^\circ \pm 18^\circ$ (nearly uniform positive polarity), $t_0 = 2009.09 \pm 0.30$ and a transition time $\tau = 0.56 \pm 0.33$ years. The polarity increased monotonically from that of a 2-sector pattern to that of a unipolar zone from 2007.00 to 2010.27.

A histogram of the polarity of \mathbf{B} observed by *V2* during four successive intervals: SW (2007.00 - 2007.67), A (2007.67 - 2008.21), B (2008.21 - 2008.83), C (2008.83 - 2009.57), and D (2009.57 - 2010.27) is shown in Figure 2(b). Here, the polarity in percent is defined as the ratio of the number of days with positive ("away") polarity ($180^\circ < \lambda < 360^\circ$) to the total number of days in each interval. Thus, from 2007.00 to 2007.67 the polarity was $+52 \pm 5\%$, corresponding to the magnetic field pointing in the "away" direction nearly half of the time and in the "toward" direction the rest of the time. In region D, from 2009.57 to 2010.27 the polarity was $+94 \pm 5\%$, as expected for magnetic fields with predominantly positive magnetic polarity in a flow from the South polar coronal hole.

The magnetic field strength profile observed by *V2* from 2007.00 to 2010.27 is shown Figure 2(c). At the TS, the daily averages of B do not appear to change significantly, although high-resolution observations show a jump in $B = 1.7 \pm 0.1$ at one of the termination shock crossings (TS-3) observed by Burlaga et al. (2008). During the rest of interval A, there were large fluctuations in B , possibly related to the TS. This interval containing strong, disturbed magnetic fields was followed by interval B and interval C in which the amplitudes of the fluctuations of B were moderate. The large amplitude fluctuations of the magnetic field strength during interval A and the moderate amplitude fluctuations during interval B and a part of interval C were discussed by Burlaga et al. (2010). Figure 2(c) shows that the amplitudes of the fluctuations in B during interval D, when *V2* was in the unipolar zone, were relatively small.

Abrupt changes in the character of the fluctuations in the plasma density and speed were discussed by Richardson & Wang (2010), who suggested that the changes are related to the turning of the heliosheath flow toward the tail. Roelof et al. (2010) attributed the decrease in the amplitude of the plasma fluctuations to the retreat of an equatorial extension of lobes of the southern polar coronal hole, the corresponding absence of corotating streams at the latitude of *V2*. Burlaga et al. (2003) calculated the radial evolution of corotating streams and their associated corotating interaction regions (CIRs) and corotating merged interaction regions (CMIRs) from 1 AU to 95 AU. They found that the amplitude of the interaction regions diminished significantly and the structure of the interaction regions increased in complexity beyond ≈ 20 AU. Thus, it is difficult to understand why the interaction regions should produce fluctuations of B with moderate

amplitudes and the heliosheath. However, a study of the interaction of CMIRs with the TS is needed to determine how the corresponding fluctuations would appear in the heliosheath.

Finally, we shall compare the distribution of λ in the sector zone with the distribution of λ in the unipolar zone. The distribution of all daily averages of λ in the sector zone during the intervals B and C is shown in Figure 3(a) and the corresponding distribution of λ in the unipolar zone during interval D is shown in Figure 3(b). There are 4 notable features of the distributions in each of these 2 panels. 1) The peaks of the distributions occur near $\lambda = 90^\circ$ and 270° . 2) There appears to be in excess of observations near 180° . 3) The peaks with positive polarity are skewed. 4) The number of days in the regions of positive magnetic polarity is greater than the number of days in the regions of negative magnetic polarity. Features 1- 3 must be interpreted with great care, since they are strongly influenced by the limitations of the observations. The angles are computed from trigonometric functions using the measured components of \mathbf{B} , and each of these components has an uncertainty of approximately 0.03 nT. Thus, the uncertainty in λ can be very large, especially when the magnetic field strength is weak. When $B < 0.04$ nT, λ is indeterminate. Even when B is strong, λ has a large uncertainty when elevation angle δ is large, and λ is undefined when $\delta = 90^\circ$. The two peaks in the λ -distribution at 90° and 270° are primarily a consequence of our assumption that $\langle BR \rangle_{52} = 0$.

Figure 3(a) and Figure 3(b) show the distributions of λ in the sector zone during intervals B and C and during interval D, respectively for the subset of observations with relatively strong magnetic fields, $B > 0.08$ nT. The peaks near 90° and 270° occur because of our assumption that $\langle BR \rangle_{52} = 0$. When only strong magnetic fields are considered, the artificial excess of observations near $\lambda = 180^\circ$ is significantly diminished, the widths of the

peaks are narrower, and the skewness is different than that observed for the set of all observations of B .

Despite the large uncertainties in the λ -distribution, one can obtain a good estimate of the fraction of days with positive polarity and the fraction of days with negative polarity, which is the principal concern of this paper. This estimate does not depend strongly on either the strength of the magnetic field or the assumption that $\langle BR \rangle_{52} = 0$. In the sector zone during intervals B and C, one can clearly see both the positive and negative polarities with a predominance of positive polarities for $B > 0.08$ nT. In the unipolar zone D, it is clear that there is nearly a uniform positive polarity with only a trace of days with negative polarity.

3. DISTRIBUTIONS OF B IN THE SECTOR ZONE AND UNIPOLAR ZONE

It is of interest to make a quantitative comparison of the distribution of the magnetic field strength observed in the unipolar zone with that observed in the sector zone.

Let us first consider the distribution of the fraction of the 503 daily averages of B versus B during intervals B and C, when V_2 was in the sector zone. This distribution is shown by the points in Figure 4(a). The error bars shown in this figure on the statistical errors in accounting rates; they do not include systematic errors which can be important, especially when $B < 0.05$ nT.

A fit of the observed distribution of B to the lognormal distribution, $y = y_0 + A/(\sqrt{(2\pi) \times w \times B}) \times \exp(-(\ln(B/B_c))^2/(2 w^2))$, shown by the solid curve in Figure 4a, provides a very good fit to the observations ($R^2 = 0.98$). The parameters of the lognormal fit are

$y_0 = -0.007 \pm 0.008$, $B_c = 0.090 \pm 0.003$, $w = 0.476 \pm 0.032$, and $A = 0.022 \pm 0.001$. Owing to the uncertainties in the measurements, a Gaussian distribution,

$y = y_0 + (A/[(w \times \sqrt{(\pi/2)})] \times \exp\{-2[(B - B_c)/w]^2\}$, shown by the dashed curve in Figure 4(a), is also consistent with the observations within the uncertainties ($R^2 = 0.89$). The parameters of this Gaussian fit are $y_0 = 0.002 \pm 0.002$, $B_c = 0.091 \pm 0.002$, $w = 0.061 \pm 0.003$, and $A = 0.0176 \pm 0.0009$. The skewness of the distribution of the daily averages of B is $K = 1.4$. Qualitatively and quantitatively, the lognormal distribution is a somewhat better fit to the observations than the Gaussian distribution.

The distribution of the fraction of the 253 daily averages of B versus B during interval D, when V_2 was in the unipolar zone, is shown in Figure 4(b). In this case, the distribution appears to be symmetric. A fit of the observed distribution of B in the unipolar zone to the Gaussian distribution shown by the solid curve in Figure 4(b) provides an excellent fit to the observations, with $R^2 = 0.99$. The parameters of the fit are $y_0 = -0.0094 \pm 0.012$, $B_c = 0.088 \pm 0.002$, $w = 0.067 \pm 0.005$, and $A = 0.022 \pm 0.002$.

4. DISTRIBUTIONS OF INCREMENTS OF B IN THE SECTOR ZONE AND UNIPOLAR ZONE

Previous studies (e. g., Burlaga & Ness, 2010) have shown that the distribution of increments of B , $dB_n(t; \tau) \equiv B(t + \tau_n) - B(t)$ on a scale of $\tau_n = 2^n$ times the unit of time, where $n = 0, 1, 2, 3, \dots$ is described by the symmetric Tsallis distribution of nonextensive statistical mechanics (Tsallis, 1988, 2004, 2009):

$R_q = A_q [1 + (q - 1)\beta_q (dB_n)^2]^{-1/(q-1)}$. The parameter q , $-\infty < q \leq 3$, is the “entropic index,” or the “nonextensivity parameter” (Tsallis 1988). The entropic index q is primarily a

measure of the size of the tails of the distribution. The parameter $w_q \equiv \beta^{-1/2}$ is primarily a measure of the width of the core of the distribution. A_q , B_q , and β_q depend on scale. The Tsallis distribution is proportional to the “q-exponential function”

$\exp_q[-\beta u] \equiv [1 + (q - 1) \beta u]^{1/(1-q)}$ where β and q are constants. As discussed by Burlaga et al. (2010), this function plays a role in the generalized central limit theorem that is analogous to the role of the exponential function $\exp(-u^2)$ in the classical central limit theorem (Umarov et al., 2008). Previous studies (e. g. Burlaga & Ness, 2010; Burlaga et al., 2010) showed that Tsallis distributions of $dBn(t)$ are observed in the heliosheath both when the distribution of $B(t)$ is lognormal and when it is Gaussian.

We shall compare the distribution of $dB0$ in the sector zone (intervals B and C) with the distribution $dB0$ measured in the unipolar zone (interval D) considering only the increments on a scale of 1 day, $\tau_0 = 1$. Figure 5(a) shows the distribution of increments of daily averages of B , $dB0$, observed in the sector zone during intervals B and C (solid squares). Figure 5(b) shows the distribution $dB0$ observed in the unipolar zone during interval D (solid squares). The distribution of $dB0$ in the sector zone appears to be more sharply peaked and has broader tails than the distribution of $dB0$ in the unipolar zone.

The solid curve in Figure 5(a) is the fit of the Tsallis distribution Rq , Equation (1), to the distribution of $dB0$ derived from the $V2$ observations of $B(t)$ in the sector zone that is plotted as the solid squares in Figure 5(a). The fit was obtained using the Levenberg–Marquardt algorithm (Levenberg 1944; Marquardt 1963). The quality of the fit, measured by the coefficient of determination $R^2 = 0.99$, is excellent. The width of the core is $w = \beta^{-1/2} = [1 / (1260 \pm 130)]^{-1/2} = (0.028 \pm 0.001)$ nT. The nonextensivity parameter derived from

the fit is $q = 1.66 \pm 0.01$. This value of q is comparable to that frequently observed in the solar wind (Burlaga & Viñas, 2005) and in the heliosheath (Burlaga et al., 2006, 2007). This value of q indicates that the large-scale fluctuations were intermittent on scales of $\tau = 1$ day in the sector zone.

The solid curve in Figure 5(b) is the fit of the Tsallis distribution R_q to the distribution of $dB0$ derived from the *V2* observations in the sector zone, interval D. The quality of the fit, measured by the coefficient of determination $R^2 = 0.96$, is again excellent. The width of the core of the distribution in the unipolar zone, $w = \beta^{-1/2} = [1 / (529 \pm 136)]^{-1/2} = (0.043 \pm 0.001)$ nT, is significantly broader than that observed in the sector zone $w = (0.028 \pm 0.001)$ nT. The nonextensivity index q is $q = 1.01 \pm 0.29$, indicating that the distribution of $dB0$ in the unipolar zone is a Gaussian function, in contrast to the non-Gaussian distribution observed in the sector zone.

5. SUMMARY AND DISCUSSION

We have shown that *Voyager 2* (*V2*) observed the polarity of the Heliosheath magnetic field change from a sector pattern with nearly equal positive and negative polarities (during "Interval SW" from 2007.00 to 2007.67) to a pattern with nearly uniform positive magnetic polarity (during the "Interval D" from 2009.57 to 2010.27). This changing polarity pattern with associated with the decreasing latitudinal width of the "sector zone" (the region containing the heliospheric current sheet) as solar activity decreased during solar cycle 23. *V2* observed the region of nearly uniform positive magnetic polarity ("the unipolar zone") associated with magnetic fields from the South

polar coronal hole, when the minimum latitudinal extent of the sector zone moved below the latitude of $V2$.

Voyager 2 was in the supersonic solar wind during Interval SW, and it crossed the termination shock at 2007.67. Thus, $V2$ was in the heliosheath most of the time during the interval under consideration. There was an interval following TS in which the magnetic field was strong and highly disturbed, possibly as a consequence of the proximity of $V2$ to the TS. Excluding this interval, there was an interval from 2008.21 to 2009.57 in which $V2$ was in the sector zone in the heliosheath, which was followed by the interval from 2009.57 to 2010.27 in which $V2$ was in the unipolar zone in the heliosheath.

We compared the distribution of daily averages of B and distribution of daily B observed in the unipolar zone with the corresponding distributions observed in the sector zone. The distribution of B in the unipolar zone was Gaussian whereas the distribution in the sectors was weakly lognormal, probably a consequence of the larger amplitudes of the fluctuations in the sector zone. The distribution of the daily increments of B in the unipolar zone was Gaussian (a Tsallis distribution, or equivalently a q -Gaussian distribution, with $q \approx 1$). In contrast, the distribution of daily increments of B in the sector zone was the Tsallis distribution with $q = 1.66 \pm 0.10$. Thus, the fluctuations of B in the sector zone are intermittent, as observed previously in the sector zone by *Voyager 1* and *Voyager 2*. We conclude that the fluctuations of B in the unipolar zone were in an equilibrium state, in contrast to the non-equilibrium fluctuations of B in the sector zone. T. McClanahan and S. Kramer provided support for the processing of the data. Daniel Berdichevsky computed the zero level offsets for the instruments. N. F. Ness was partially

supported by NASA Grants NASA NNX 07AW09G and NASA NNX 09AT41G to the Catholic University of America.

REFERENCES

Ahluwalia, H.S. & Ygbuhay, R. C. 2011, *Advances in Space Research* doi:
10.1016/j.asr2011.01.003 (in press)

Borovikov, S. N., Pogorelov, N. V., Burlaga, L. F., and Richardson, J. D. 2011, *ApJ*, 728, L21,
doi:10.1088/2041-8205/728/1/L21

Burlaga, L. F., & Ness, N. F. 1997, *J. Geophys. Res.*, 102, A9, 19,731 – 19,742

Burlaga, L. F., & Ness, N. F. 2003, *J. Geophys. Res.*, 108, NO. A10, 8028,
doi:10.1029/2003JA009870

Burlaga, L. F. & Ness, N. F., 2010, *ApJ*, 725, 1306-1316

Burlaga, L. F., Wang, C., Richardson, J. D., & Ness, N. F. 2003, *ApJ.*, 590(1), 554–566,
doi:10.1086/374926.

Burlaga, L. F., Ness, N. F., Acuña, M. H., Lepping, R. P., Connerney, J. E. P., & Richardson, J. D.
2008, *Nature*, 454, doi:10.1038/nature07029

Burlaga, L. F. , Ness, N. F., Acuña, M. H., Richardson, J. D., Stone, E. C. , & McDonald, F. B.
2009, ApJ, 692, 1125-1130 doi: 10.1088/0004-637X/692/2/1125

Burlaga, L. F., Ness, N. F., Wang, Y.- M., Sheeley, N. R., & Richardson, J. D. 2010, J. Geophys.
Res., 115 doi:10.1029/2009JA015239

Burlaga, L. F., & Viñas, A. 2005, Physica A, 356, 375

Burlaga, L. F., Viñas, A., Ness, N. F., & Acuña, M. H. 2006, ApJ, 644, L83

Burlaga, L. F., Viñas, A., & Wang, C. 2007, J. Geophys. Res., 112, A07206

Levenberg, K. 1944, Quart. Appl. Math., 2, 164

Marquardt, D. 1963, SIAM J. Appl. Math., 11, 431

Ness, N. F., & Burlaga, L. F. 2001, J. Geophys. Res., 106, 15, 803-15, 818,
doi:10.1029/2000JA000118

Parker, E. N. 1963, Interplanetary Dynamical Processes (New York: Interscience)

Richardson, J. D., & Wang, C. 2010, ApJ Lett., 711, L44–L47

Roelof, E. C., Decker, R. B., & Krimigis, S. M. 2010, AIP Conf. Proc., 1216, 359–362

Schatten, K. H., Wilcox, J. M., & Ness, N. F. 1969, *Solar Physics*, 6, 442-445, doi: 10.1007/BF00146478

Shultz, M. 1973, *Astrophysics and Space Science*, 24, 371-383, doi: 10.1007/BF02637162.

Smith, E. J. 2001, *J. Geophys. Res.*, 106, 15819-15831, doi: 10.1029/2000JA 000120.

Tsallis, C. 1988, *J. Stat. Phys.*, 52, 479

Tsallis, C. 2004, in *Nonextensive Entropy-Interdisciplinary Applications*, ed. M. Gell-Mann & C. Tsallis (New York: Oxford Univ. Press)

Tsallis, C. 2009, *Introduction to Nonextensive Statistical Mechanics* (New York: Springer)

Umarov, S., Tsallis, C., & Steinberg, S. 2008, *Milan J. Math.*, 76, 307

Wang, Y.-M., & Sheeley, N. R. Jr. 1992, *ApJ*, 392, 310-319, doi: 10.1086/171430.

FIGURE CAPTIONS

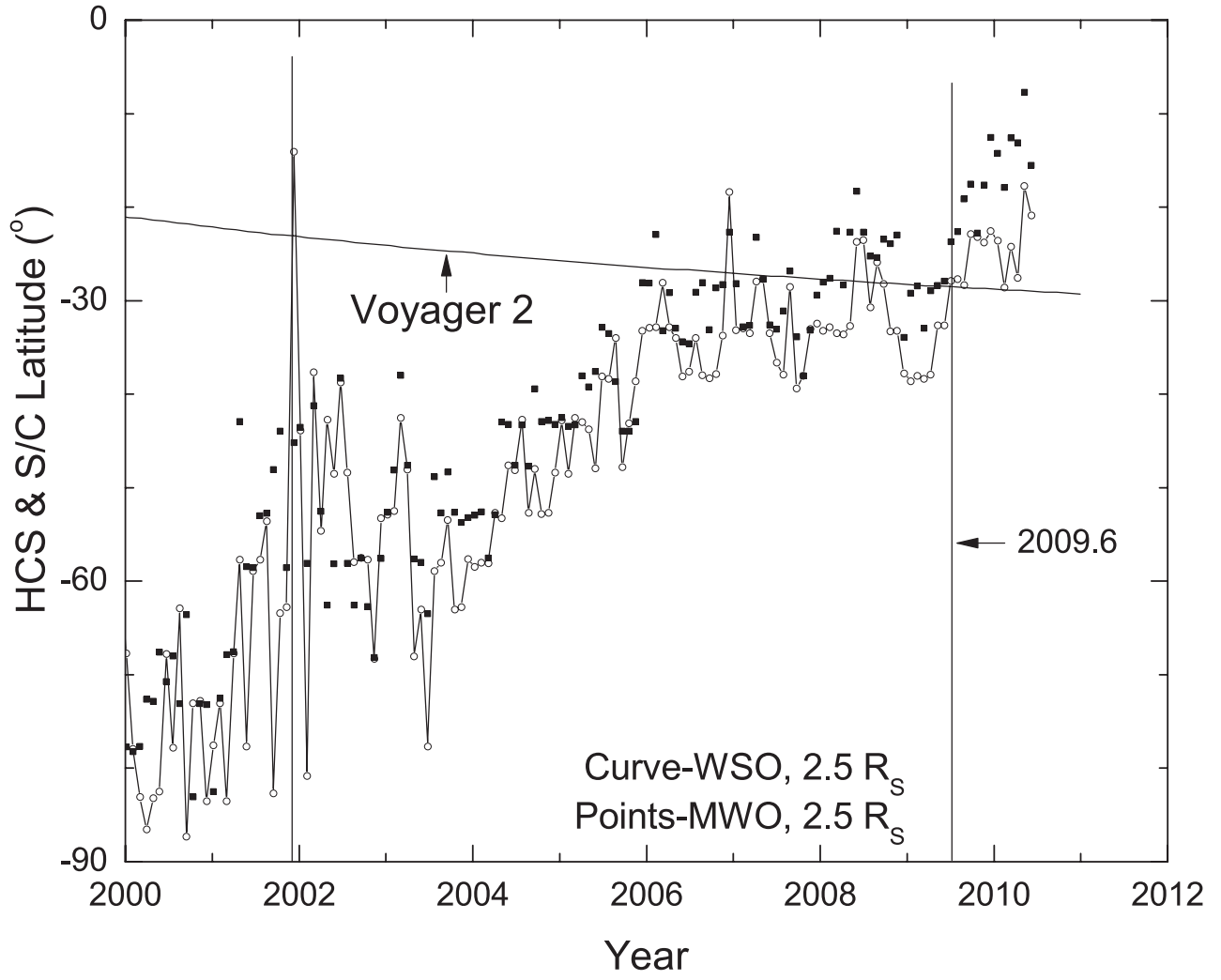
Figure 1. The minimum latitudinal extent of heliosphere current sheet computed from the "radial model" with a source surface at 2.5 solar radii, with data from the Wilcox Solar Observatory (WSO) and the Mount Wilson Observatory (MWO). The latitude of *V2* is shown by the nearly straight curve.

Figure 2. (a) Daily averages of the azimuthal angle of the magnetic field λ measured by Voyager 2. (b) Histograms of the magnetic polarity. (c) Daily averages of the magnetic field strength.

Figure 3. Distributions of the daily averages of the azimuthal angle λ (a) for all of the data in the sector zone, intervals B and C and (b) for all of the data in the unipolar zone, interval D. Distributions of the daily averages of the azimuthal angle λ (c) for the data with $B > 0.08$ nT in the sector zone and (d) for the data with $B > 0.08$ nT in the unipolar zone

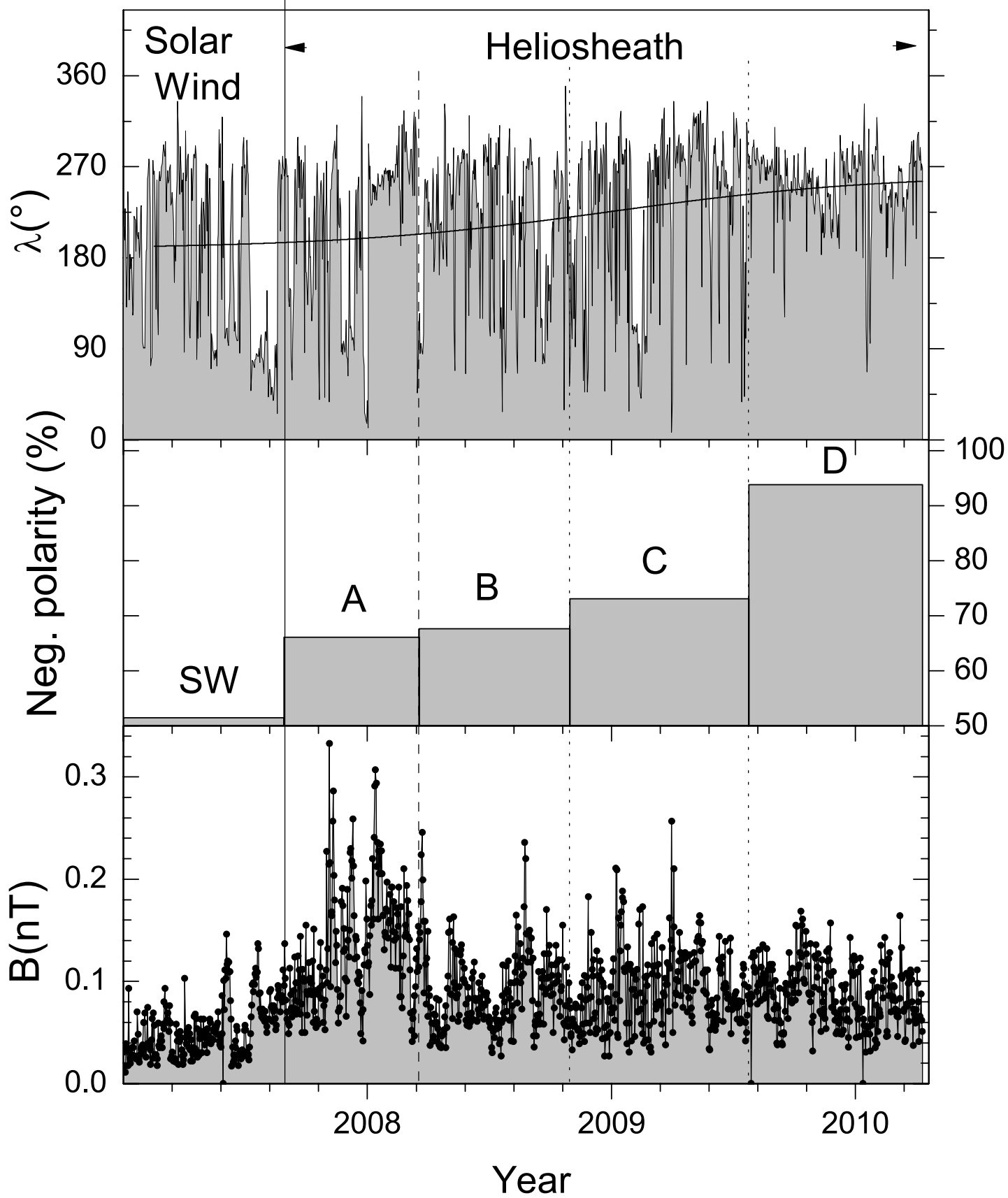
Figure 4. Distributions of daily averages of the magnetic field strength B observed by *V2* (solid squares) in the heliosheath in (a) the sector zone during intervals B and C and in (b) the unipolar zone during interval D. The curves in these figures are least squares fit to the data.

Figure 5. (a) Distribution of increments of daily averages of B, dB0, in the sector zone during intervals B and C (solid squares together with the fit of the Tsallis distribution to the solid squares shown by the solid curve). (b) Distribution of increments dB0 and the unipolar zone during interval D (solid squares) together with the fit of the Tsallis distribution to the solid squares shown by the solid curve.

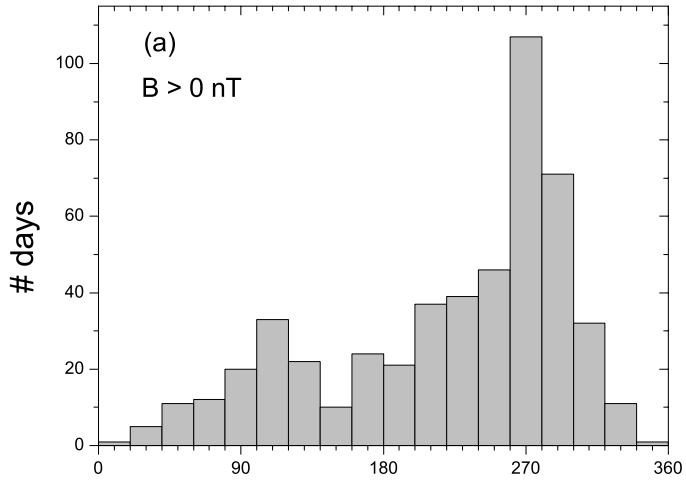


TS

Voyager 2



Intervals B & C



Interval D

